Aerospace Science and Technology 78 (2018) 452–460

Contents lists available at ScienceDirect

Aerospace Science and Technology

www.elsevier.com/locate/aescte

Virtual-command-based model reference adaptive control for abrupt structurally damaged aircraft

Jing Zhang, Xiaoke Yang, Lingyu Yang *

School of Automation Science and Electrical Engineering, Beihang University, Beijing, 100191, China

A R T I C L E I N F O

Article history:
Received 7 February 2018
Received in revised form 26 April 2018
Accepted 28 April 2018
Available online 1 May 2018

Keywords:
Abrupt structurally damaged aircraft
Flight safety
Adaptive control
Transient performance improvement

A B S T R A C T

Although a high-gain learning rate can offer ideal tracking performance in adaptive control in theory, it can also lead to high-frequency oscillations in practice due to the unmodeled dynamics of the system. In aircraft structural damage scenarios, the strong uncertainty and the safety-critical nature of the problem make this conflict critical. In this paper, a novel virtual-command-based model reference adaptive control (MRAC) scheme for flight control is proposed. In the new framework, the direct relationship between the learning law and the actual tracking error is broken; instead, a virtual command is introduced as the input to the standard MRAC controller. The key feature is that even when the virtual tracking error is large, the actual tracking error can be maintained within a small range; thus, the MRAC learning rate does not necessarily need to be large to suppress the virtual transient tracking error, which is greatly beneficial for the robustness of the MRAC controller. The proposed method is illustrated by the attitude control of the 6-DOF nonlinear Generic Transport Model in a scenario with a broken left wing tip.

1. Introduction

Structural damage to the airframe of a modern aircraft, such as structural failure in the wing tip, vertical tail or engine, is one of the most serious threats that pilots face. Such structural damage may lead to significant, abrupt and non-symmetric uncertainties in the aircraft aerodynamics, mass properties, and control efficiencies [1,2]. The control responses of such a damaged aircraft can be far different from those of normal aircraft [3–5]. Consequently, a fundamental problem arising in flight control theory is to ensure the recovery of stability and the level of desired performance when significant abrupt changes in uncertainties occur.

Compared with fixed-gain robust control design approaches, adaptive control methods more effectively address these sources of uncertainty and require less modeling information; thus, they have gradually gained popularity. A variety of adaptive control approaches have been proposed to address the strong uncertainty caused by structural damage [6–10]. These early studies mainly focused on large uncertainties and theoretical guarantees of asymptotic stability. However, little attention has been paid to the transient performance when abrupt variations occur. Unfortunately, due to the nonlinear and complex aerodynamics, poor transient performance can contribute to fatal accidents:

1) A poor transient response can excite unmodeled dynamics and/or place the aircraft under dangerous conditions, such as stall or spin [11,12].

2) The use of a high learning rate in adaptive control may result in high-frequency oscillations, which can violate actuator rate saturation constraints and excite unmodeled system dynamics [13].

Because the standard model reference adaptive control (MRAC) learning law directly relies on the tracking error, it usually has poor transient performance in the learning phase [14]. Before the stable region is reached, this undesired transient response can be far from the reference signal [15]. Improvement of the transient performance is thus a challenging practical topic in adaptive control.

A classic approach is to modify the reference model [16,11,17,18]. A closed-loop reference model (CRM) structure was proposed in [16,11], in which plant information was used to alter the reference trajectory to improve the transient properties. [17] introduced a new reference system to prevent the update law from attempting to learn from high-frequency system error content. Because the CRM approach does not introduce new information to the controller, i.e., the learning process is still driven by the tracking error, it can be treated as a nonlinear adjustment to the learning rate.

The transient performance can also be improved by adjusting the learning law. [19] and [20] modified the adaptive learning law in accordance with an upper bound or a prescribed performance bound on the desired transient performance. [21] and [22] used nonlinear generalized restricted potential functions to maintain

* Corresponding author.
E-mail address: yanglingyu@buaa.edu.cn (L. Yang).

https://doi.org/10.1016/j.ast.2018.04.043
1270-9638/

Nomenclature

$\alpha_i(\boldsymbol{\lambda})$ scheduling coefficient for the ith vertex
$\bar{\alpha}$ angle of attack .... deg
$\bar{\beta}$ sideslip angle .... deg
$\boldsymbol{\Gamma}_\delta \in \mathbb{R}_+^{m\times m}$ symmetric positive-definite learning matrix of $\boldsymbol{\delta}$
$\boldsymbol{\Gamma}_\phi \in \mathbb{R}_+^{(l-1+m)\times(l-1+m)}$ symmetric positive-definite learning matrix of $\boldsymbol{\phi}$
$\boldsymbol{\lambda} \in \mathbb{R}^{n_\lambda}$ vector of structural damage
ω bandwidth of the learning error observer
ϕ roll angle .... deg
ψ yaw angle .... deg
$\sigma_{\max}(\cdot)$ maximum eigenvalues of the matrix
$\sigma_{\min}(\cdot)$ minimum eigenvalues of the matrix
θ pitch angle .... deg
$\boldsymbol{A}(\boldsymbol{\lambda}) \in \mathbb{R}^{n\times n}$ system matrix
$\boldsymbol{A}_i \in \mathbb{R}^{n\times n}$ vertices of the convex hull
$\boldsymbol{A}_m \in \mathbb{R}^{n\times n}$ system matrix of the reference model
$\boldsymbol{B}(\boldsymbol{\lambda}) \in \mathbb{R}^{n\times m}$ control input matrix
$\boldsymbol{B}_m \in \mathbb{R}^{n\times m}$ control input matrix of the reference model
$\boldsymbol{d}(\boldsymbol{\lambda}) \in \mathbb{R}^{m}$ disturbance
$\boldsymbol{D} \in \mathbb{R}^{n\times m}$ disturbance input matrix
$\boldsymbol{e}_r \in \mathbb{R}^{n}$ actual tracking error
$\boldsymbol{e}_v \in \mathbb{R}^{n}$ virtual tracking error
$\boldsymbol{q} \in \mathbb{R}^{m}$ learning error of the adaptive control system
$\boldsymbol{r} \in \mathbb{R}^{m}$ reference command/actual command
$\boldsymbol{u} \in \mathbb{R}^{m}$ input vector
$\boldsymbol{v} \in \mathbb{R}^{m}$ virtual command
$\boldsymbol{x} \in \mathbb{R}^{n}$ state vector
$\boldsymbol{x}_{m_r} \in \mathbb{R}^{n}$ actual reference state vector
$\boldsymbol{x}_{m_v} \in \mathbb{R}^{n}$ virtual reference state vector
$\boldsymbol{\Lambda}(\boldsymbol{\lambda}) \in \mathbb{R}^{m\times m}$ control effectiveness matrix
H altitude .... m
p roll rate .... deg/s
q pitch rate .... deg/s
r yaw rate .... deg/s
t time .... s
t_d time of the damage .... s
u_e, u_a, u_r deflections (deg) of the elevator, aileron and rudder
v airspeed .... m/s
X north position .... m
Z east position .... m

the transient performance error below an a priori, user-defined worst-case closed-loop system performance bound. [23] developed a derivative-free adaptive control law and showed that its robustness against unmodeled dynamics is improved by increasing the adaptation gain. [14] added a mismatch estimation term to suppress high-frequency oscillations. [24] proposed a bi-objective optimal control modification method that establishes a tradeoff between performance and robustness through the suitable selection of the modification parameters. [25] introduced an artificial basis function to minimize the system tracking error during the learning phase of an adaptive controller. [26] presented a novel architecture that includes modification terms in the adaptive controller and the learning law; these modification terms vanish as the system reaches its steady state. In addition to the above approaches, [27–32] investigated the problem of improving the transient performance for specific systems.

In the existing methods, the transient performance is improved by modifying the reference model and/or the learning law; however, these methods still follow the basic MRAC scheme, i.e., the learning laws are driven by the tracking error. The tradeoff between a large transient tracking error and a high learning rate remains a problem. From a practical standpoint, a high learning rate may lead to control saturation, control oscillation or the excursion of control components outside of the linear regime, among other undesirable effects, and the learning rate cannot be increased to an unlimited extent. To solve this problem, this paper proposes a novel approach in which the direct relationship between the learning law and the closed-loop tracking error is broken; instead, a virtual command and a virtual tracking error are used to drive the learning law. The proposed control scheme has the following features: 1) The virtual command works on both the reference model and the controller but does not involve any modification of the reference model, the update law or the controller, especially the learning rate. Thus, the virtual command does not affect the stability, robustness or error convergence properties of the standard MRAC scheme, and it can be applied in combination with most MRAC methods. 2) The virtual tracking error can be large while the actual tracking error is maintained within a small range; thus, the MRAC learning rate does not necessarily need to be large to suppress the virtual transient tracking error, which is greatly beneficial for the robustness of the MRAC controller. 3) The virtual command is designed to compensate for the learning error instead of the MRAC tracking error. Note that the learning error is related to the time derivative of the tracking error; thus, compensating for the learning error is more efficient.

The remainder of this paper is organized as follows. Section 2 introduces the model of a damaged aircraft. Section 3 presents a standard linear-parameter-varying-model-based model reference adaptive control scheme (LPV-MRAC). Section 4 analyzes the transient performance of LPV-MRAC. A new approach, called virtual-command-based MRAC (VC-MRAC), is proposed in Section 5 to improve the transient performance. A simulation of the generic transport model (GTM) in a scenario in which the left wing tip has broken off is discussed in Section 6. Finally, conclusions are given in Section 7.

2. Plant models and problem formulation

In this paper, a linear parameter-varying (LPV) model is used to represent the dynamics of a structurally damaged aircraft as follows:

$$\dot{\boldsymbol{x}} = \boldsymbol{A}(\boldsymbol{\lambda})\boldsymbol{x} + \boldsymbol{B}(\boldsymbol{\lambda})\boldsymbol{u} + \boldsymbol{D}\boldsymbol{d}(\boldsymbol{\lambda}), \tag{1}$$

where $\boldsymbol{D}$ is a known disturbance input matrix; and $\boldsymbol{A}(\boldsymbol{\lambda})$, $\boldsymbol{B}(\boldsymbol{\lambda})$ and $\boldsymbol{d}(\boldsymbol{\lambda})$ are functions of an unknown parameter vector $\boldsymbol{\lambda}$, which represents the severity of various types of damage, such as a broken-off wing tip, a broken-off vertical tail and a broken-off left stabilizer.

Considering that aircraft damage occurs instantaneously, $\boldsymbol{\lambda}$ is formulated as a function that shows switching behavior at a specific time, that is,

$$\boldsymbol{\lambda}(t) = \begin{cases} \boldsymbol{\lambda}_0, t < t_d \\ \boldsymbol{\lambda}_d, t \geq t_d \end{cases}. \tag{2}$$

Note that an aircraft is a physical system, and $\boldsymbol{\lambda}$ can be assumed to be bounded such that $\boldsymbol{\lambda} \in \Omega_\lambda$. Therefore, $\boldsymbol{A}(\boldsymbol{\lambda})$ must lie in a compact set that can be embedded in a polytope, that is,

$$\boldsymbol{A}(\boldsymbol{\lambda}) = \sum_{i=1}^{l} \alpha_i(\boldsymbol{\lambda})\boldsymbol{A}_i, \tag{3}$$

where the $\boldsymbol{A}_i$ correspond to the vertices of the convex hull $\mathrm{Co}\{\boldsymbol{A}_1,\ldots,\boldsymbol{A}_l\}$ and $\alpha_i(\boldsymbol{\lambda})$ is the scheduling coefficient for the ith vertex. The $\alpha_i(\boldsymbol{\lambda})$ satisfy the following conditions:

$$\alpha_i(\boldsymbol{\lambda}) \geq 0 \; (i=1,\ldots,l), \tag{4a}$$

$$\sum_{i=1}^{l} \alpha_i(\boldsymbol{\lambda}) = 1. \tag{4b}$$

Considering that the control efficiency may be affected by the damage, the control input matrix is formulated as

$$\boldsymbol{B}(\boldsymbol{\lambda}) = \boldsymbol{D}\boldsymbol{\Lambda}(\boldsymbol{\lambda}), \tag{5}$$

where $\boldsymbol{\Lambda}(\boldsymbol{\lambda}) \in \mathbb{R}^{m\times m}$ is an unknown positive diagonal control effectiveness matrix related to $\boldsymbol{\lambda}$.

In addition to the uncertainties in the system matrix and input matrix, $\boldsymbol{d}(\boldsymbol{\lambda})$ is introduced to represent the strong disturbance caused by the damage, and it is assumed to be a piecewise and slowly time-varying function. As is standard, we also assume that $\det(\boldsymbol{D}^\top \boldsymbol{D}) \neq 0$ and that each pair $(\boldsymbol{A}_i, \boldsymbol{D})$ is controllable.

Remark 1. Eq. (1) can be transformed into a general form as in [17,24,16]. The differences are that we use a polytopic LPV model to represent the system dynamics with uncertainty and that the vertex matrices are obtained via a higher-order singular value decomposition procedure [33].

Next, the desired reference model with respect to $\boldsymbol{r}$ is given by

$$\dot{\boldsymbol{x}}_{m_r} = \boldsymbol{A}_m \boldsymbol{x}_{m_r} + \boldsymbol{B}_m \boldsymbol{r}. \tag{6}$$

The goal is to design an adaptive controller for the system described by Eq. (1) to track the reference model given in Eq. (6) while maintaining an acceptable transient performance.

3. LPV-MRAC scheme

In this section, an LPV-MRAC controller is presented based on the standard MRAC design procedure. In particular, a virtual command $\boldsymbol{v}$ is introduced as the input to the LPV-MRAC controller instead of the actual input $\boldsymbol{r}$. Correspondingly, $\boldsymbol{e}_r \triangleq \boldsymbol{x} - \boldsymbol{x}_{m_r}$ and $\boldsymbol{e}_v \triangleq \boldsymbol{x} - \boldsymbol{x}_{m_v}$ are defined as the actual and virtual tracking errors, respectively, and $\boldsymbol{x}_{m_v}$ is the virtual reference state given by

$$\dot{\boldsymbol{x}}_{m_v} = \boldsymbol{A}_m \boldsymbol{x}_{m_v} + \boldsymbol{B}_m \boldsymbol{v}. \tag{7}$$

The design of $\boldsymbol{v}$ will be discussed in a later section. To track the virtual reference model given in Eq. (7), an ideal feedback control law is formulated by taking the inverse of Eq. (1), i.e.,

$$\boldsymbol{u} = \boldsymbol{\Lambda}^{-1}\left(-\sum_{i=1}^{l} \alpha_i \boldsymbol{K}_{1_i}\boldsymbol{x} + \boldsymbol{K}_2\boldsymbol{v} - \boldsymbol{d}\right), \tag{8}$$

where $\boldsymbol{K}_{1_i}$ and $\boldsymbol{K}_2$ satisfy

$$\boldsymbol{D}\boldsymbol{K}_{1_i} = \boldsymbol{A}_i - \boldsymbol{A}_m, \; (i=1\ldots l) \text{ and } \boldsymbol{D}\boldsymbol{K}_2 = \boldsymbol{B}_m. \tag{9}$$

By combining the known terms into $\boldsymbol{\theta}_i \triangleq (-\boldsymbol{K}_{1_i}\boldsymbol{x} + \boldsymbol{K}_2\boldsymbol{v}) \in \mathbb{R}^m$ $(i = 1\ldots l)$, Eq. (8) is converted to

$$\boldsymbol{u} = \boldsymbol{\Lambda}^{-1}\left(\sum_{i=1}^{l} \alpha_i \boldsymbol{\theta}_i - \boldsymbol{d}\right). \tag{10}$$

By further defining $\boldsymbol{\Theta} \triangleq [\boldsymbol{\theta}_2 - \boldsymbol{\theta}_1, \boldsymbol{\theta}_3 - \boldsymbol{\theta}_1, \ldots, \boldsymbol{\theta}_l - \boldsymbol{\theta}_1, -\boldsymbol{I}_m] \in \mathbb{R}^{m\times(l-1+m)}$, $\boldsymbol{\phi} \triangleq [\alpha_2, \alpha_3, \ldots, \alpha_l, \boldsymbol{d}^\top]^\top \in \mathbb{R}^{l-1+m}$ and $\boldsymbol{\Delta} \triangleq \boldsymbol{\Lambda}^{-1}$, the constraint in Eq. (4a) can be incorporated into the ideal control law as follows:

$$\boldsymbol{u} = \boldsymbol{\Delta}(\boldsymbol{\theta}_1 + \boldsymbol{\Theta}\boldsymbol{\phi}). \tag{11}$$

Since $\boldsymbol{\Delta}$ and $\boldsymbol{\phi}$ are unknown, the actual control law is formulated by using their estimates, as follows:

$$\boldsymbol{u} = \hat{\boldsymbol{\Delta}}\left(\boldsymbol{\theta}_1 + \boldsymbol{\Theta}\hat{\boldsymbol{\phi}}\right). \tag{12}$$

By substituting Eq. (12) into Eq. (1), an expression for the closed-loop system dynamics is obtained:

$$\dot{\boldsymbol{x}} = \boldsymbol{A}_m\boldsymbol{x} + \boldsymbol{B}_m\boldsymbol{v} + \boldsymbol{D}\boldsymbol{\Theta}\tilde{\boldsymbol{\phi}} + \boldsymbol{D}\boldsymbol{\Lambda}\tilde{\boldsymbol{\Delta}}\left(\boldsymbol{\theta}_1 + \boldsymbol{\Theta}\hat{\boldsymbol{\phi}}\right), \tag{13}$$

where $\tilde{\boldsymbol{\Delta}} \triangleq \hat{\boldsymbol{\Delta}} - \boldsymbol{\Delta}$ and $\tilde{\boldsymbol{\phi}} \triangleq \hat{\boldsymbol{\phi}} - \boldsymbol{\phi}$ are the estimated errors on $\boldsymbol{\Delta}$ and $\boldsymbol{\phi}$, respectively. Thus, the virtual tracking error dynamics are obtained by subtracting Eq. (7) from Eq. (13) as follows:

$$\dot{\boldsymbol{e}}_{\boldsymbol{v}} = \boldsymbol{A}_m\boldsymbol{e}_{\boldsymbol{v}} + \boldsymbol{D}\boldsymbol{\Theta}\tilde{\boldsymbol{\phi}} + \boldsymbol{D}\mathrm{diag}(\boldsymbol{\theta}_1 + \boldsymbol{\Theta}\hat{\boldsymbol{\phi}})\boldsymbol{\Lambda}\tilde{\delta}, \tag{14}$$

where δ is a column vector formed from the diagonal elements of $\boldsymbol{\Delta}$ and diag() returns a square diagonal matrix with the elements of the input vector on the main diagonal. Then, the adaptive laws for the unknown parameters are chosen as follows:

$$\begin{aligned} \dot{\hat{\delta}} &= -\boldsymbol{\Gamma}_\delta \mathrm{diag}\left(\boldsymbol{\theta}_1 + \boldsymbol{\Theta}\hat{\boldsymbol{\phi}}\right)(\boldsymbol{P}\boldsymbol{D})^\top \boldsymbol{e}_{\boldsymbol{v}}, \\ \dot{\hat{\boldsymbol{\phi}}} &= -\boldsymbol{\Gamma}_\phi \boldsymbol{\Theta}^\top (\boldsymbol{P}\boldsymbol{D})^\top \boldsymbol{e}_{\boldsymbol{v}}, \end{aligned} \tag{15}$$

where $\boldsymbol{P} \in \mathbb{R}^{n\times n}$ is a solution of the Lyapunov equation

$$\boldsymbol{A}_m^\top \boldsymbol{P} + \boldsymbol{P}\boldsymbol{A}_m + \boldsymbol{Q} = \boldsymbol{0}, \tag{16}$$

where $\boldsymbol{Q}$ is a symmetric positive-definite real matrix. Now, we choose the Lyapunov function

$$V(\boldsymbol{e}_{\boldsymbol{v}}, \tilde{\delta}, \tilde{\boldsymbol{\phi}}) = \boldsymbol{e}_{\boldsymbol{v}}^\top \boldsymbol{P}\boldsymbol{e}_{\boldsymbol{v}} + \tilde{\delta}^\top \boldsymbol{\Gamma}_\delta^{-1}\boldsymbol{\Lambda}\tilde{\delta} + \tilde{\boldsymbol{\phi}}^\top \boldsymbol{\Gamma}_\phi^{-1}\tilde{\boldsymbol{\phi}}. \tag{17}$$

Note that $V(\boldsymbol{0},\boldsymbol{0},\boldsymbol{0}) = 0$ and $V(\boldsymbol{e}_{\boldsymbol{v}}, \tilde{\delta}, \tilde{\boldsymbol{\phi}}) \geq 0$ for all $(\boldsymbol{e}_{\boldsymbol{v}}, \tilde{\delta}, \tilde{\boldsymbol{\phi}}) \neq (\boldsymbol{0},\boldsymbol{0},\boldsymbol{0})$. The time derivative of V is

$$\begin{aligned} &\dot{V}(\boldsymbol{e}_{\boldsymbol{v}}, \tilde{\delta}, \tilde{\boldsymbol{\phi}}) \\ &\quad= -\boldsymbol{e}_{\boldsymbol{v}}^\top \boldsymbol{Q}\,\boldsymbol{e}_{\boldsymbol{v}} + 2\left(\boldsymbol{e}_{\boldsymbol{v}}^\top \boldsymbol{P}\boldsymbol{D}\mathrm{diag}(\boldsymbol{\theta}_1 + \boldsymbol{\Theta}\hat{\boldsymbol{\phi}}) + \dot{\hat{\delta}}^\top \boldsymbol{\Gamma}_\delta^{-1}\right)\boldsymbol{\Lambda}\tilde{\delta} \\ &\qquad+ 2\left(\boldsymbol{e}_{\boldsymbol{v}}^\top \boldsymbol{P}\boldsymbol{D}\boldsymbol{\Theta} + \dot{\hat{\boldsymbol{\phi}}}^\top \boldsymbol{\Gamma}_\phi^{-1}\right)\tilde{\boldsymbol{\phi}}. \end{aligned} \tag{18}$$

Substituting Eq. (15) into Eq. (18) yields $\dot{V}(\boldsymbol{e}_{\boldsymbol{v}}, \tilde{\delta}, \tilde{\boldsymbol{\phi}}) = -\boldsymbol{e}_{\boldsymbol{v}}^\top \boldsymbol{Q}\,\boldsymbol{e}_{\boldsymbol{v}}$; in other words, the derivative of the Lyapunov function is negative unless $\boldsymbol{e}_{\boldsymbol{v}} = \boldsymbol{0}$. Since $\boldsymbol{\lambda}$, $\boldsymbol{e}_{\boldsymbol{v}}$, $\tilde{\delta}$, $\tilde{\boldsymbol{\phi}}$ and $\boldsymbol{u}$ are bounded, it follows from Eq. (14) that $\dot{\boldsymbol{e}}_{\boldsymbol{v}}$ is bounded. Then, according to Barbalat's lemma, $\ddot{V}(\boldsymbol{e}_{\boldsymbol{v}}, \tilde{\delta}, \tilde{\boldsymbol{\phi}}) = -2\dot{\boldsymbol{e}}_{\boldsymbol{v}}^\top \boldsymbol{Q}\,\boldsymbol{e}_{\boldsymbol{v}}$ is also bounded, and

$$\dot{V}(\boldsymbol{e}_{\boldsymbol{v}}, \tilde{\delta}, \tilde{\boldsymbol{\phi}}) \to 0, \tag{19}$$

which consequently shows that $\boldsymbol{e}_{\boldsymbol{v}} \to \boldsymbol{0}$ as $t \to \infty$.

4. Transient performance of LPV-MRAC

While the above LPV-MRAC method has been proven to be Lyapunov stable, the virtual tracking error is not guaranteed to be asymptotically stable and may be very large during the transient period, i.e., the learning period of the adaptive control system. In practice, a large transient tracking error may drive the aircraft into a nonlinear or unmodeled region, resulting in failure of the adaptive control law. Therefore, the tracking error must be bounded in a safe range.

By manipulating Eq. (17), it can be found that the 2-norm of $\boldsymbol{e_v}(t)$ satisfies

$$\sigma_{min}(\boldsymbol{P})\|\boldsymbol{e_v}(t)\|_2^2 \le \boldsymbol{e_v}(t)^\top \boldsymbol{P}\boldsymbol{e_v}(t) \le V(\boldsymbol{e_v}(t), \tilde{\delta}(t), \tilde{\boldsymbol{\phi}}(t)). \tag{20}$$

Note that $\dot{V}(\boldsymbol{e_v}, \tilde{\delta}\tilde{\boldsymbol{\phi}}) \le 0$ implies that

$$\begin{aligned} V(\boldsymbol{e_v}, \tilde{\delta}, \tilde{\boldsymbol{\phi}}) &\le V(\boldsymbol{e_v}(t_d), \tilde{\delta}(t_d), \tilde{\boldsymbol{\phi}}(t_d)) \\ &\le \sigma_{max}(\boldsymbol{P})\|\boldsymbol{e_v}(t_d)\|_2^2 + \|\tilde{\delta}(t_d)^\top \boldsymbol{\Gamma}_\delta^{-1/2}\boldsymbol{\Lambda}^{1/2}\|_F^2 \\ &\quad + \|\tilde{\boldsymbol{\phi}}(t_d)\boldsymbol{\Gamma}_{\boldsymbol{\phi}}^{-1/2}\|_F^2. \end{aligned} \tag{21}$$

Since $\boldsymbol{e_v}(t)$ is guaranteed to be stable and converge to zero, we can assume that $\boldsymbol{e_v}(t)$ has reached its steady state and has become zero before t_d, i.e., $\boldsymbol{e_v}(t_{d-}) = 0$. Thus, by inserting Eq. (20) into Eq. (21), the following expression for the tracking error bound is obtained:

$$\|\boldsymbol{e_v}(t)\|_2 \le \sqrt{(\|\tilde{\delta}(t_d)^\top \boldsymbol{\Gamma}_\delta^{-1/2}\boldsymbol{\Lambda}^{1/2}\|_F^2 + \|\tilde{\boldsymbol{\phi}}(t_d)\boldsymbol{\Gamma}_{\boldsymbol{\phi}}^{-1/2}\|_F^2)/\sigma_{min}(\boldsymbol{P})}. \tag{22}$$

Hence, the maximum transient error is directly related to $\boldsymbol{\Gamma}_\delta$, $\boldsymbol{\Gamma}_{\boldsymbol{\phi}}$ and $\boldsymbol{P}$. As shown by Eq. (15), increasing $\boldsymbol{\Gamma}_\delta$, $\boldsymbol{\Gamma}_{\boldsymbol{\phi}}$ or $\boldsymbol{P}$ will lead to an increase in the learning rate; i.e., the only way to decrease the transient error is to increase the learning rate. Because the learning law is directly driven by the tracking error, this problem will always exist. A novel approach is to break this relationship between the learning law and the tracking error.

5. VC-MRAC scheme

In this section, a virtual-command-based scheme is introduced to improve the transient tracking performance while maintaining the robustness of the MRAC scheme.

The transient dynamics with respect to $\boldsymbol{v}$ can be approximated by reformulating Eq. (13) as follows:

$$\dot{\boldsymbol{x}} = \boldsymbol{A}_m\boldsymbol{x} + \boldsymbol{B}_m\boldsymbol{v} + \boldsymbol{D}\boldsymbol{q}, \tag{23}$$

where $\boldsymbol{q} \triangleq \boldsymbol{\Theta}\tilde{\boldsymbol{\phi}} + \boldsymbol{\Lambda}\tilde{\boldsymbol{\Delta}}\left(\boldsymbol{\theta}_1 + \boldsymbol{\Theta}\hat{\boldsymbol{\phi}}\right)$ is defined as the learning error of the adaptive control system. In contrast to the reference model given in Eq. (7) $\boldsymbol{x}$ is driven by the learning error and may be far from the actual reference trajectory $\boldsymbol{x}_{m_r}$. The actual tracking error can be suppressed by adjusting the trajectory of $\boldsymbol{v}$ to compensate for the error dynamics caused by the learning error.

Set $\boldsymbol{\epsilon} = \boldsymbol{D}\boldsymbol{q}$ and $\dot{\boldsymbol{\epsilon}} = \boldsymbol{h}$. Considering the abruptness of the parameter variations due to the damage to the aircraft that occurs at time $t = t_d$, the following assumptions hold for $\boldsymbol{h}$:

$$\begin{cases} \boldsymbol{h}(t) = \boldsymbol{0} & t < t_d \\ \|\boldsymbol{h}(t_d)\|_2 = \infty, \int_{t_d^-}^{t_d^+} \boldsymbol{h}(t)\mathrm{d}t = \boldsymbol{\epsilon}(t_d) & t_d^- \le t \le t_d^+ \\ \sup_{t>t_d} \|\boldsymbol{h}(t)\|_2 = \bar{h} & t > t_d \end{cases}. \tag{24}$$

Thus, the learning error observer (LEO) is given by

$$\begin{cases} \dot{\hat{\boldsymbol{x}}} = \boldsymbol{A}_m\boldsymbol{x} + \boldsymbol{B}_m\boldsymbol{v} + \hat{\boldsymbol{\epsilon}} + 2\omega(\boldsymbol{x} - \hat{\boldsymbol{x}}) \\ \dot{\hat{\boldsymbol{\epsilon}}} = \omega^2(\boldsymbol{x} - \hat{\boldsymbol{x}}) \end{cases}. \tag{25}$$

Theorem 1. *For the system described by Eq. (23) and the assumptions in Eq. (24), the error of the LEO given by Eq. (25) is bounded as follows:*

$$\|\tilde{\boldsymbol{\epsilon}}(t)\|_2 \le \|\boldsymbol{\epsilon}(0)\|_2(1+\omega t)e^{-\omega\Delta t} + \frac{2\bar{h}}{\omega}, \tag{26}$$

where $\tilde{\boldsymbol{\epsilon}} \triangleq \boldsymbol{\epsilon} - \hat{\boldsymbol{\epsilon}}$ *and* $\Delta t \triangleq t - t_d$.

Proof. Let $\tilde{\boldsymbol{x}} \triangleq \boldsymbol{x} - \hat{\boldsymbol{x}}$. We then obtain

$$\begin{bmatrix} \dot{\tilde{\boldsymbol{x}}} \\ \dot{\tilde{\boldsymbol{\epsilon}}} \end{bmatrix} = \begin{bmatrix} -2\omega\boldsymbol{I}_n & \boldsymbol{I}_n \\ -\omega^2\boldsymbol{I}_n & \boldsymbol{0}_n \end{bmatrix} \begin{bmatrix} \tilde{\boldsymbol{x}} \\ \tilde{\boldsymbol{\epsilon}} \end{bmatrix} + \begin{bmatrix} \boldsymbol{0} \\ \boldsymbol{I}_n \end{bmatrix}\boldsymbol{h} = \boldsymbol{A}_o \begin{bmatrix} \tilde{\boldsymbol{x}} \\ \tilde{\boldsymbol{\epsilon}} \end{bmatrix} + \boldsymbol{B}_o\boldsymbol{h}. \tag{27}$$

Note that $\boldsymbol{A}_o$ is a block matrix and that all of its submatrices are diagonal. The matrix exponential can thus be obtained as follows:

$$e^{\boldsymbol{A}_o t} = \begin{bmatrix} (1-\omega t)e^{-\omega t}\boldsymbol{I}_n & te^{-\omega t}\boldsymbol{I}_n \\ -\omega^2 te^{-\omega t}\boldsymbol{I}_n & (1+\omega t)e^{-\omega t}\boldsymbol{I}_n \end{bmatrix}. \tag{28}$$

Then, the time-domain response of Eq. (27) can be expressed as

$$\begin{aligned} \tilde{\boldsymbol{\epsilon}}(t) &= \int_{t_d}^{t} [\boldsymbol{0}, \boldsymbol{I}_n]e^{\boldsymbol{A}_o(t-\tau)}\boldsymbol{B}_o\boldsymbol{h}(\tau)\mathrm{d}\tau \\ &= \int_{t_d}^{t} (1+\omega(t-\tau))\,e^{-\omega(t-\tau)}\boldsymbol{h}(\tau)\mathrm{d}\tau. \end{aligned} \tag{29}$$

By manipulating Eq. (24), the error dynamics can be further expressed as

$$\begin{aligned} \|\tilde{\boldsymbol{\epsilon}}(t)\|_2 &\le \|\boldsymbol{\epsilon}(t_d)\|_2(1+\omega\Delta t)e^{-\omega\Delta t} \\ &\quad + \int_{t_d^+}^{t} (1+\omega(t-\tau))e^{-\omega(t-\tau)}\bar{h}\mathrm{d}\tau \\ &= \|\boldsymbol{\epsilon}(t_d)\|_2(1+\omega\Delta t)e^{-\omega\Delta t} \\ &\quad + \frac{2\bar{h}}{\omega}(1 - e^{-\omega\Delta t} - \frac{1}{2}\omega\Delta te^{-\omega\Delta t}); \end{aligned} \tag{30}$$

therefore, Eq. (30) is a direct consequence of Eq. (26) because $1 - e^{-\omega\Delta t} - \frac{1}{2}\omega\Delta te^{-\omega\Delta t} \le 1$ for $\Delta t \ge 0$. □

Remark 2. Eq. (29) implies that $\tilde{\epsilon}_i(t) = \int_{t_d}^{t}(1+\omega_i(t-\tau)) \times e^{-\omega_i(t-\tau)}h_i(\tau)\mathrm{d}\tau$ and $\epsilon_i(t) = \int_{t_d}^{t} h_i(t)\mathrm{d}t$. It follows that $|\tilde{\epsilon}_i(t)/\epsilon_i(t)| \le 1$ and $\left\|\tilde{\boldsymbol{\epsilon}}(t)\right\|_2 \le \|\boldsymbol{\epsilon}(t)\|_2$.

Remark 3. According to Eq. (30), the upper bound on the observer's error is inversely proportional to ω, and the bound's convergence rate is proportional to ω. Thus, the observer's performance can be improved by increasing ω. On the other hand, the convergence speed of the adaptive control law in Eq. (14) is limited by the reference model dynamics, which means that the LEO could be more effective than the adaptive control law when ω is sufficiently large.

On the basis of the observer given in Eq. (25), the virtual command $\boldsymbol{v}$ is given by

$$\boldsymbol{v} = -\boldsymbol{B}_m^+\hat{\boldsymbol{\epsilon}} + \boldsymbol{r}, \tag{31}$$

where $\boldsymbol{B}_m^+$ is the pseudoinverse of $\boldsymbol{B}_m$ and $\boldsymbol{r}$ is the actual control command.

Note that $\boldsymbol{\epsilon} = \boldsymbol{B}_m\boldsymbol{K}_2^{-1}\boldsymbol{q} = \boldsymbol{B}_m(\boldsymbol{B}_m^+\boldsymbol{B}_m)\boldsymbol{K}_2^{-1}\boldsymbol{q} = \boldsymbol{B}_m\boldsymbol{B}_m^+\boldsymbol{\epsilon}$; thus, applying Eq. (31) to the system described by Eq. (13) yields

$$\dot{\boldsymbol{x}} = \boldsymbol{A}_m\boldsymbol{x} + \boldsymbol{B}_m(\boldsymbol{r} - \boldsymbol{B}_m^+\hat{\boldsymbol{\epsilon}}) + \boldsymbol{B}_m\boldsymbol{B}_m^+\boldsymbol{\epsilon} = \boldsymbol{A}_m\boldsymbol{x} + \boldsymbol{B}_m\boldsymbol{r} + \boldsymbol{B}_m\boldsymbol{B}_m^+\tilde{\boldsymbol{\epsilon}}. \tag{32}$$

By subtracting Eq. (6) from Eq. (32), the following expression for the actual tracking error is obtained:

$$\boldsymbol{e_r}(t) = \boldsymbol{A}_m\boldsymbol{e_r} + \boldsymbol{B}_m\boldsymbol{B}_m^+\tilde{\boldsymbol{\epsilon}}, \tag{33}$$

which yields

$$\boldsymbol{e_r}(t) = \int_0^t e^{\boldsymbol{A}_m(t-\tau)} \boldsymbol{B}_m \boldsymbol{B}_m^{+} \tilde{\boldsymbol{\epsilon}}(\tau)\mathrm{d}\tau, \ (t \geq 0). \tag{34}$$

Since $\boldsymbol{A}_m$ is a Hurwitz matrix, the following upper bound holds [34]:

$$\|e^{\boldsymbol{A}_m t}\|_2 \leq \beta e^{-\omega_{\boldsymbol{H}} t}, \tag{35}$$

where $\omega_{\boldsymbol{H}} = -1/\sigma_{\max}(\boldsymbol{H})$, $\beta = \sqrt{\sigma_{\max}(\boldsymbol{H})/\sigma_{\min}(\boldsymbol{H})}$, and $\boldsymbol{H}$ is the solution to

$$\boldsymbol{A}_m^\top \boldsymbol{H} + \boldsymbol{H}\boldsymbol{A} = -2\boldsymbol{I}_n. \tag{36}$$

Note that $\|\boldsymbol{B}_m \boldsymbol{B}_m^{+}\|_2 = \|\boldsymbol{B}_m^{+}\boldsymbol{B}_m\|_2 = 1$, which leads to $\|\boldsymbol{B}_m \boldsymbol{B}_m^{+}\tilde{\boldsymbol{\epsilon}}(t)\|_2 \leq \|\tilde{\boldsymbol{\epsilon}}(t)\|_2$. Furthermore, substituting Eq. (35) and Eq. (26) into Eq. (34) yields

$$\begin{aligned}\|\boldsymbol{e_r}(t)\|_2 \leq & \int_{t_d}^t \beta e^{-\omega_{\boldsymbol{H}}(t-\tau)} \|\boldsymbol{B}_m \boldsymbol{B}_m^{+}\|_2 \|\tilde{\boldsymbol{\epsilon}}(\tau)\|_2 \mathrm{d}\tau \\ & \leq \beta \|\boldsymbol{\epsilon}(t_d)\|_2 e^{-\omega_{\boldsymbol{H}}\Delta t} \left\{ \frac{1}{\omega - \omega_{\boldsymbol{H}}} \left(1 - e^{-(\omega-\omega_{\boldsymbol{H}})\Delta t}\right) \right. \\ & \left. + \frac{\omega}{(\omega-\omega_{\boldsymbol{H}})^2} \left(1 - (1 + (\omega - \omega_{\boldsymbol{H}})\Delta t)\, e^{-(\omega-\omega_{\boldsymbol{H}})\Delta t}\right) \right\} \\ & + \frac{2\beta}{\omega\omega_{\boldsymbol{H}}} \bar{h}(1 - e^{-\omega_{\boldsymbol{H}}\Delta t}).\end{aligned} \tag{37}$$

To improve the transient performance, the bandwidth of the LEO must be greater than the reference bandwidth, i.e., $\omega - \omega_{\boldsymbol{H}} > 0$. Then, Eq. (37) can be further rewritten as follows:

$$\|\boldsymbol{e_r}(t)\|_2 \leq \beta \frac{2\omega - \omega_{\boldsymbol{H}}}{(\omega - \omega_{\boldsymbol{H}})^2} \|\boldsymbol{\epsilon}(t_d)\|_2 e^{-\omega_{\boldsymbol{H}}\Delta t} + \frac{2\beta}{\omega_{\boldsymbol{H}}\omega}\bar{h}. \tag{38}$$

It is now straightforward to see that the maximum transient error can be suppressed by increasing the bandwidth of the LEO.

6. Application to the generic transport model

6.1. The GTM and the control objective

To illustrate the proposed adaptive control scheme, we conducted simulations of the GTM with the left wing tip broken, as shown in Fig. 1. The nonlinear aerodynamic coefficients of aircraft with left wing-tip damage (0 to 33% semi-span) are provided in Ref. [35]. The dynamics of such an aircraft are described by the following general nonlinear ordinary differential equation:

$$\dot{\mathbb{X}} = \boldsymbol{f}(\mathbb{X}, \boldsymbol{u}, \boldsymbol{\lambda}), \tag{39}$$

where $\mathbb{X} \triangleq [v, \bar{\alpha}, q, \theta, H, \bar{\beta}, p, r, \phi, \psi, X, Z]^\top \in \mathbb{R}^{12}$ is the state vector. Our goal is to design an attitude controller that can track a predesigned reference model while maintaining acceptable transient performance. The state vector is chosen to be $\boldsymbol{x} = [\theta, \phi, \psi, q, p, r]^\top$, and the desired reference model of the attitude dynamics is given by

$$\boldsymbol{A}_m = \begin{bmatrix} \boldsymbol{0}_3 & \boldsymbol{I}_3 \\ -\omega_m^2 \boldsymbol{I}_3 & -2\xi_m\omega_m \boldsymbol{I}_3 \end{bmatrix}, \boldsymbol{B}_m = \begin{bmatrix} \boldsymbol{0}_3 \\ \omega_m^2 \boldsymbol{I}_3 \end{bmatrix}, \tag{40}$$

where $\omega_m = 5$ rad/s and $\xi_m = 0.7$ are chosen to provide the desired handling characteristics.

Fig. 1. NASA generic transport model.

The uncertainties and disturbances are as follows:

1) The system dynamics vary with damage, as reported in Ref. [35], and the approximate polytopic model presented in the following subsection describes the variation of the system matrix.

2) The control efficiency uncertainty induced by the damage is $\boldsymbol{\Lambda}(t) = \mathrm{diag}([0.6, 0.8, 0.7])(t > t_d)$.

3) The disturbance vector is defined as $\boldsymbol{d} = \boldsymbol{d}_0 + \boldsymbol{d}_D$, where $\boldsymbol{d}_0$ is an unknown constant offset caused by the structural damage (approximately $[0.0003, -5.5895, 0.1921]^\top$ in the 20% left wing-tip damage scenario) and $\boldsymbol{d}_D$ is a vector function of time given by

$$\boldsymbol{d}_D(t) = \begin{bmatrix} 0.2\mathrm{e}^{-0.5\Delta t}\sin 0.4\Delta t - 0.2\sin 0.6\Delta t\cos 0.4\Delta t \\ 0.3\mathrm{e}^{-0.5\Delta t}\sin 0.6\Delta t - 0.2\sin 0.4\Delta t\cos 0.6\Delta t \\ 0.3\mathrm{e}^{-0.5\Delta t}\sin 0.6\Delta t - 0.2\sin 0.4\Delta t\cos 0.6\Delta t \end{bmatrix} (t \geq t_d). \tag{41}$$

4) To make the illustration more practical, two kinds of unmodeled dynamics are considered. The dynamics of the remaining terms of $\mathbb{X}$, such as $\bar{\alpha}$, $\bar{\beta}$ and v, are treated as unmodeled uncertainties and are assumed to be stable. In addition, the actuator dynamics are considered to be high-frequency unmodeled dynamics, i.e., a second-order system with a damping ratio of 0.7 and a natural frequency of 70 rad/s.

The LPV-MRAC scheme and the proposed VC-MRAC scheme are evaluated based on the above nonlinear GTM.

6.2. LPV-MRAC performance evaluation

An LPV-MRAC scheme was designed for the operating point of $v = 45.3$ m/s, $\bar{\alpha} = 4.096$ deg, $H = 304.8$ m and $\boldsymbol{u} = [1.77, 0, 0]^\top$ deg. By means of a higher-order singular value decomposition procedure [33], the attitude dynamics with broken-off wing-tip damage ranging from 0 to 33% of the semi-span can be approximated by an LPV model with 3 vertices as follows:

$$\boldsymbol{A}_1 = \begin{bmatrix} 0 & 0 & 0 & 1.0000 & 0 & 0 \\ 0 & 0 & 0 & 0 & 1.0000 & 0.0716 \\ 0 & 0 & 0 & 0 & 0 & 1.0026 \\ 0 & 0 & 0 & -3.0363 & 0.0002 & -0.0001 \\ 0 & 0 & 0 & 0.0017 & -4.6607 & 0.5483 \\ 0 & 0 & 0 & 0.0001 & -0.3936 & -1.0178 \end{bmatrix},$$

$$\boldsymbol{A}_2 = \begin{bmatrix} 0 & 0 & 0 & 1.0000 & 0 & 0 \\ 0 & 0 & 0 & 0 & 1.0000 & 0.0716 \\ 0 & 0 & 0 & 0 & 0 & 1.0026 \\ 0 & 0 & 0 & -3.0040 & -0.1347 & 0.0062 \\ 0 & 0 & 0 & -0.5039 & -3.2178 & 0.4940 \\ 0 & 0 & 0 & -0.0508 & -0.2770 & -1.0287 \end{bmatrix},$$

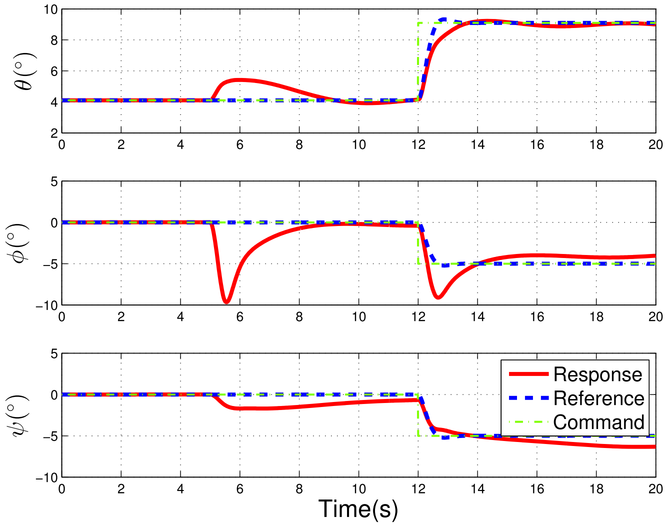

(a) Attitude response.

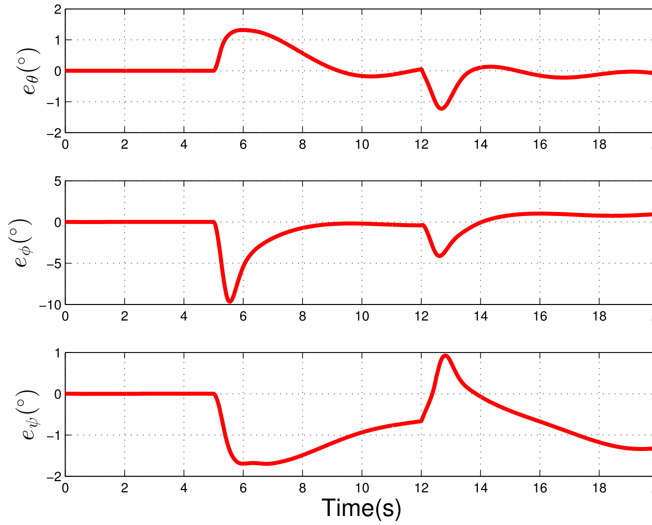

(b) Attitude tracking error response.

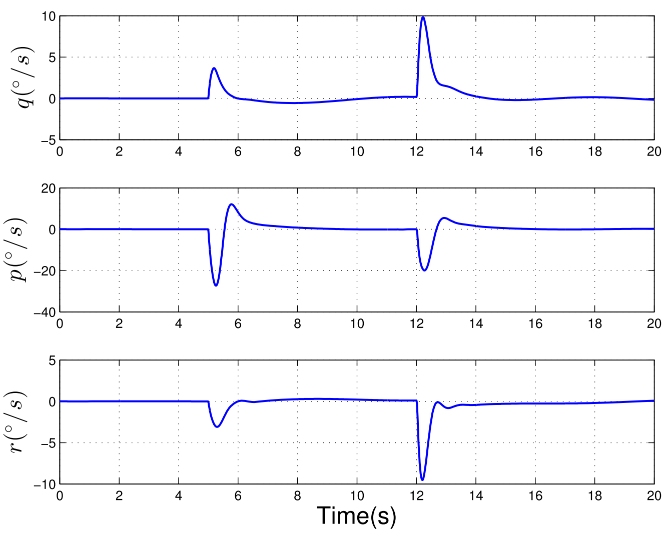

(c) Attitude rate response.

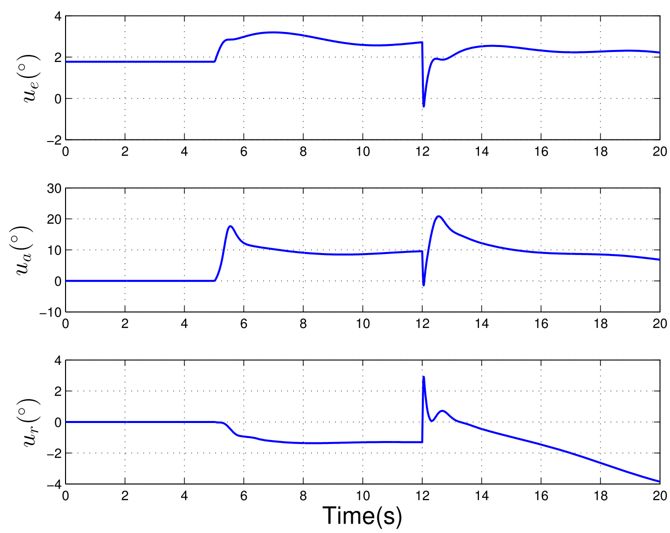

(d) Actuator response.

Fig. 2. LPV-MRAC results for 20% broken-off wing-tip damage and a step command.

$$\boldsymbol{A}_3 = \begin{bmatrix} 0 & 0 & 0 & 1.0000 & 0 & 0 \\ 0 & 0 & 0 & 0 & 1.0000 & 0.0716 \\ 0 & 0 & 0 & 0 & 0 & 1.0026 \\ 0 & 0 & 0 & -3.0247 & -0.0499 & 0.0022 \\ 0 & 0 & 0 & 0.0102 & -4.6630 & 0.5506 \\ 0 & 0 & 0 & -0.0003 & -0.3955 & -1.0208 \end{bmatrix},$$

$$\boldsymbol{B} = \boldsymbol{D} = \begin{bmatrix} 0 & 0 & 0 \\ 0 & 0 & 0 \\ 0 & 0 & 0 \\ -43.2677 & 0 & 0 \\ 0 & 39.5905 & 11.1467 \\ 0 & 3.2841 & -28.5431 \end{bmatrix}. \tag{42}$$

The other parameter settings are listed in Table 1.

A 20-second simulation with step attitude commands was conducted, as illustrated in Fig. 2. An event causing 20% damage to the left wing tip was assumed to occur 5 s after the start of the simulation; then, a step command was issued at 12 s. Fig. 2 shows the attitude response and tracking error. The attitude response tracks the command, but the transient error can still be improved.

Table 1
Controller parameter settings.

Parameter	Setting
$\mathbf{Q}$	diag([3 3 3 0.3 0.3 0.3])
$\boldsymbol{\Gamma}_{\phi}$	diag([0.1 0.1 0.1 0.1 0.1])
$\boldsymbol{\Gamma}_{\delta}$	diag([0.01 0.01 0.01])

Next, we show how the learning rate affects the controller's performance. The values of the learning matrices were increased to k times their original values given in Table 1. Fig. 3 shows that when there are no unmodeled actuator dynamics, a higher learning rate results in better tracking performance, i.e., a smaller maximum tracking error and a faster convergence speed. However, this finding does not always hold when actuator dynamics are added into the system. As shown in Fig. 4, the system starts to oscillate at $k = 35$ and becomes unstable at k greater than 35, which indicates that the robustness of the standard MRAC scheme to the unmodeled dynamics is reduced with an increasing learning rate.

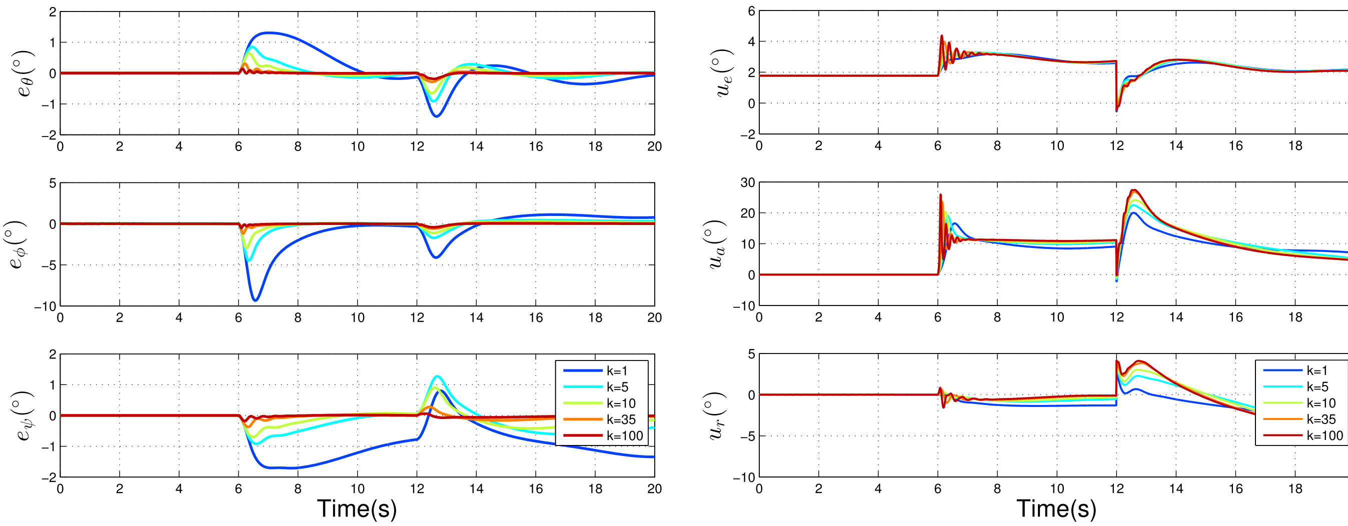

(a) Attitude tracking error response. (b) Actuator response.

Fig. 3. LPV-MRAC tracking performance for 20% broken-off wing-tip damage and a step command (for varying learning rates without unmodeled dynamics).

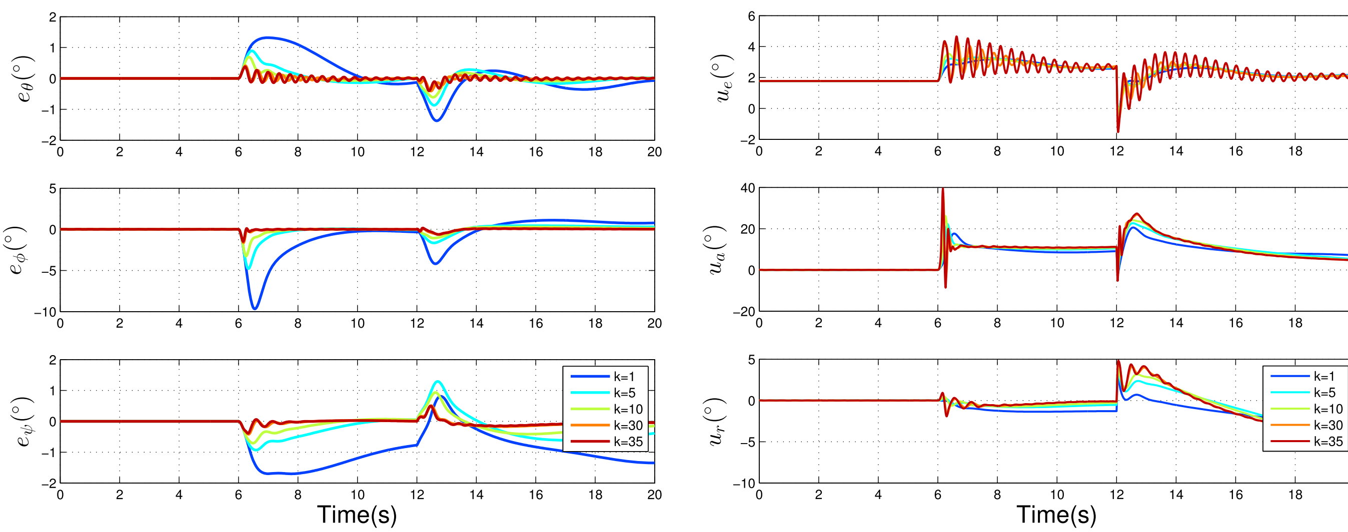

(a) Attitude tracking error response. (b) Actuator response.

Fig. 4. LPV-MRAC tracking performance for 20% broken-off wing-tip damage and a step command (for varying learning rates with unmodeled dynamics).

6.3. VC-MRAC performance evaluation

We now show how the VC-MRAC scheme affects the tracking performance. The learning matrices were chosen as shown in Table 1, and the unmodeled dynamics were also included in the simulation.

Fig. 5 shows the tracking error as ω increases. The transient performance is greatly improved, and the actuator responses are smooth.

Fig. 6 shows the VC-MRAC response with $\omega = 30$ and $k = 1$. As shown in Fig. 6(a), the attitude tracks the reference model well. Fig. 6(b) shows that $\boldsymbol{e}_r$ decreases rapidly and that the maximum roll angle error is less than 2 deg. In addition, the convergence speed of the virtual tracking error is relatively slow, and the maximum virtual tracking error reaches 8 deg in the roll channel. Fig. 6(c) and (d) show that the actuator deflections are smooth and within the constraints and that the coupled effects on safety-critical states, such as the airspeed, angle of attack and sideslip angle, are also very small.

7. Conclusion

To achieve high transient performance in the event of abrupt and severe structural damage to an aircraft, a virtual-command-based model reference adaptive control (VC-MRAC) scheme was proposed. In comparison with the classic approach, a virtual command and a virtual tracking error were introduced to break the direct relationship between the learning law and the actual tracking error. The design process for the virtual command controller and the learning error observer were further studied in detail. A system-theoretical analysis and illustrative numerical examples were presented to demonstrate that the new approach is effective in maintaining high tracking performance with improved robustness compared with the standard MRAC scheme. Future research will include studies on the application of the proposed scheme in combination with other adaptive control approaches and in nonlinear systems.

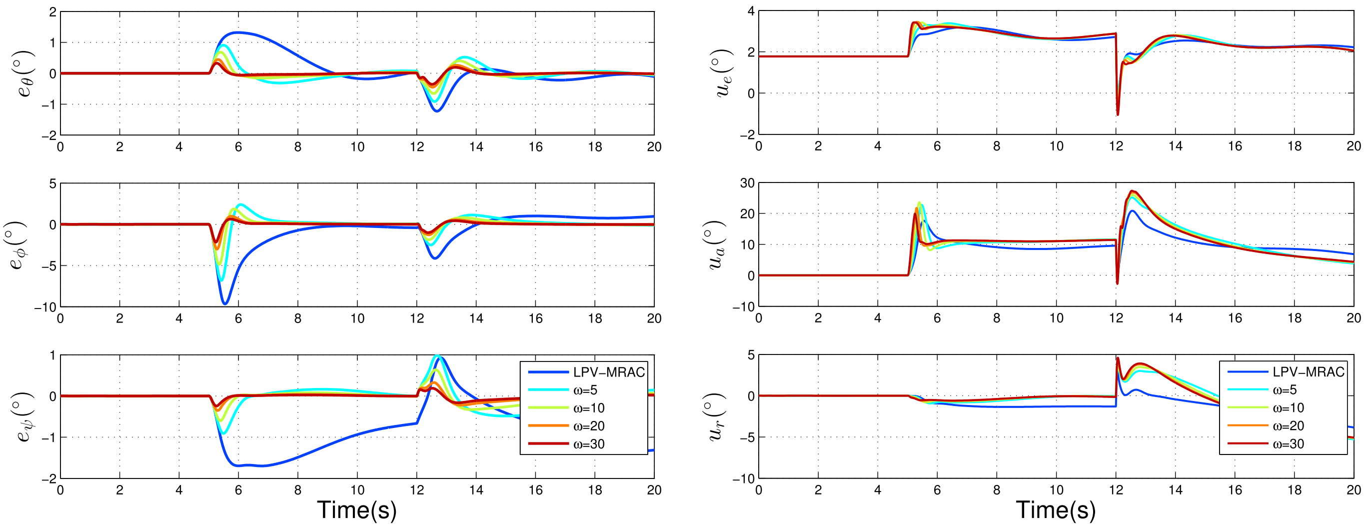

(a) Attitude tracking error response.
(b) Actuator response.

Fig. 5. VC-MRAC controller outputs for 20% broken-off wing-tip damage and a step command (with varying ω).

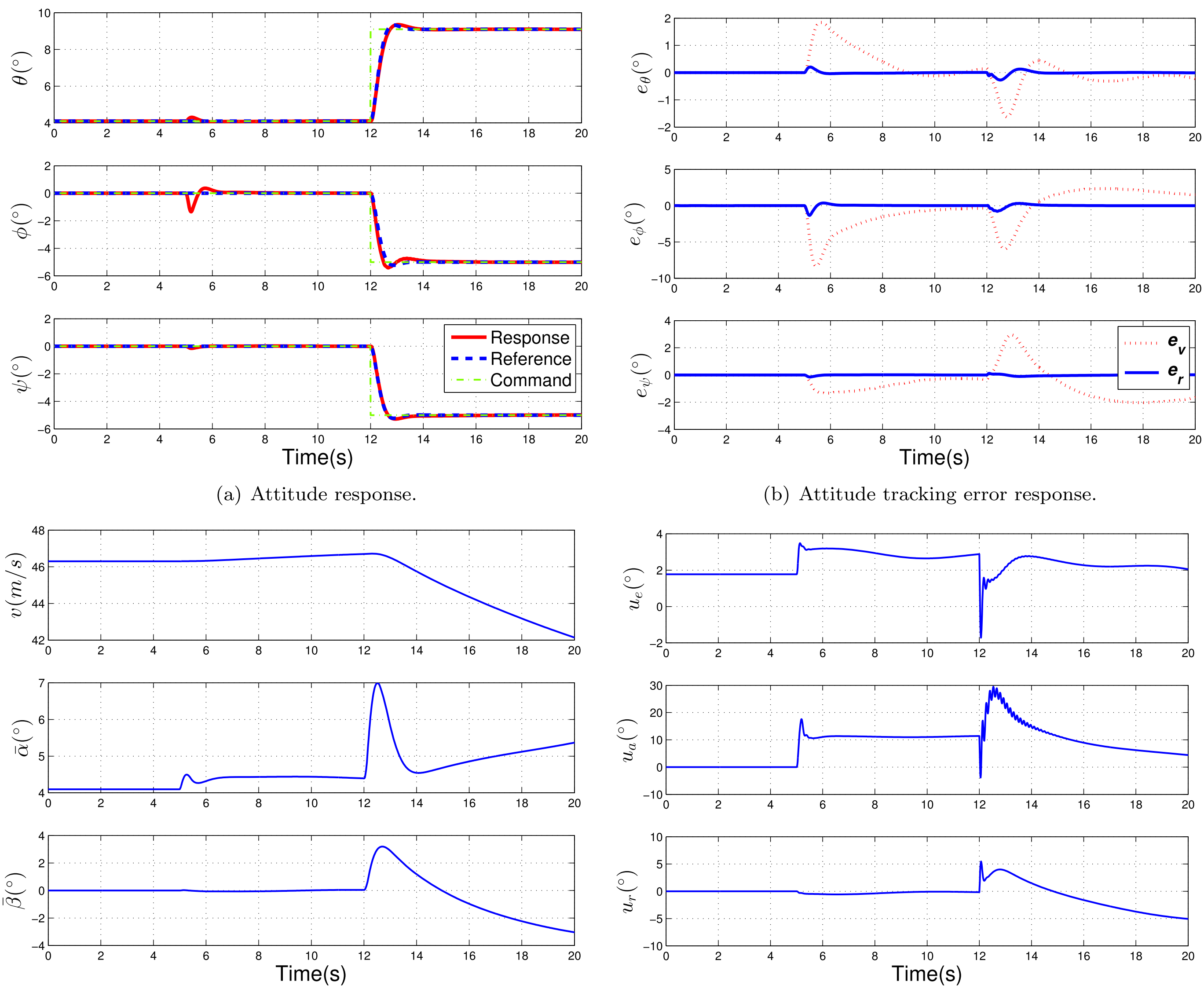

(a) Attitude response.
(b) Attitude tracking error response.
(c) Other state responses.
(d) Actuator response.

Fig. 6. VC-MRAC tracking performance for 20% broken-off wing-tip damage and a step command (with $\boldsymbol{\omega} = 30$).

Conflict of interest statement

None declared.

Acknowledgements

This research was funded by the National Natural Science Foundation of China (Grant Nos. 61273099 and 61304030).

References

[1] N. Nguyen, K. Krishnakumar, J. Kaneshige, P. Nespeca, Flight dynamics and hybrid adaptive control of damaged aircraft, J. Guid. Control Dyn. 31 (3) (2008) 751–764, https://doi.org/10.2514/1.28142.

[2] P. Stojakovic, B. Rasuo, Minimal safe speed of the asymmetrically loaded combat airplane, Aircr. Eng. Aerosp. Technol. 88 (1) (2016) 42–52, https://doi.org/10.1108/AEAT-03-2014-0033.

[3] Aviation Safety, Statistical Summary Of Commercial Jet Airplane Accidents, Tech. Rep., Boeing Commercial Airplanes, Seattle, Washington, USA, July 2016.

[4] J. White, Aviation safety program, NASA.

[5] P. Stojakovic, K. Velimirovic, B. Rasuo, Power optimization of a single propeller airplane take-off run on the basis of lateral maneuver limitations, Aerosp. Sci. Technol. 72 (2018) 553–563, https://doi.org/10.1016/j.ast.2017.10.015.

[6] N.T. Nguyen, K. Krishnakumar, Hybrid intelligent flight control with adaptive learning parameter estimation, J. Aerosp. Comput. Inf. Commun. 6 (3) (2009) 171–186, https://doi.org/10.2514/1.35929.

[7] V. Stepanyan, S. Campbell, K. Krishnakumar, Adaptive control of a damaged transport aircraft using M-MRAC, in: AIAA Guidance, Navigation, and Control Conference, 2010, pp. 1–19.

[8] Y. Liu, G. Tao, S.M. Joshi, Modeling and model reference adaptive control of aircraft with asymmetric damage, J. Guid. Control Dyn. 33 (5) (2010) 1500–1517, https://doi.org/10.2514/6.2009-5617.

[9] J. Guo, G. Tao, Y. Liu, Multivariable adaptive control of NASA generic transport aircraft model with damage, J. Guid. Control Dyn. 34 (5) (2011) 1495–1506, https://doi.org/10.2514/1.53258.

[10] J. Guo, G. Tao, A discrete-time multivariable MRAC scheme applied to a nonlinear aircraft model with structural damage, Automatica 53 (2015) 43–52, https://doi.org/10.1016/j.automatica.2014.12.036.

[11] T. Gibson, Z. Qu, A. Annaswamy, E. Lavretsky, et al., Adaptive output feedback based on closed-loop reference models, IEEE Trans. Autom. Control 60 (10) (2015) 2728–2733, https://doi.org/10.1109/TAC.2015.2405295.

[12] P. Stojakovic, B. Rasuo, Single propeller airplane minimal flight speed based upon the lateral maneuver condition, Aerosp. Sci. Technol. 49 (2016) 239–249, https://doi.org/10.1016/j.ast.2015.12.012.

[13] Z.T. Dydek, A.M. Annaswamy, E. Lavretsky, Adaptive control and the NASA X-15-3 flight revisited, IEEE Control Syst. 30 (3) (2010) 32–48, https://doi.org/10.1109/MCS.2010.936292.

[14] S.h. Kim, Y. Kim, Mismatch-observer based model reference adaptive control for transient performance improvement of aircraft, in: AIAA Guidance, Navigation, and Control Conference, 2017, pp. 1–12.

[15] X. Yu, Y. Zhang, Z. Liu, Fault-tolerant flight control design with explicit consideration of reconfiguration transients, J. Guid. Control Dyn. 38 (12) (2015) 556–563, https://doi.org/10.2514/1.G001414.

[16] T. Gibson, A. Annaswamy, E. Lavretsky, Improved transient response in adaptive control using projection algorithms and closed loop reference models, in: AIAA Guidance, Navigation, and Control Conference, 2012, pp. 1–13.

[17] T. Yucelen, G. De La Torre, E.N. Johnson, Improving transient performance of adaptive control architectures using frequency-limited system error dynamics, Int. J. Control 87 (11) (2014) 2383–2397, https://doi.org/10.1080/00207179.2014.922702.

[18] R. Dey, S.K. Jain, P.K. Padhy, Robust closed loop reference MRAC with PI compensator, IET Control Theory Appl. 10 (18) (2016) 2378–2386, https://doi.org/10.1049/iet-cta.2016.0430.

[19] W. Sun, Y. Zhang, Y. Huang, H. Gao, O. Kaynak, Transient-performance-guaranteed robust adaptive control and its application to precision motion control systems, IEEE Trans. Ind. Electron. 63 (10) (2016) 6510–6518, https://doi.org/10.1109/TIE.2016.2542787.

[20] W. Wang, C. Wen, Adaptive actuator failure compensation control of uncertain nonlinear systems with guaranteed transient performance, Automatica 46 (12) (2010) 2082–2091, https://doi.org/10.1016/j.automatica.2010.09.006.

[21] E. Arabi, B.C. Gruenwald, T. Yucelen, J.E. Steck, Guaranteed model reference adaptive control performance in the presence of actuator failures, in: AIAA Information Systems-AIAA Infotech@ Aerospace, 2017, pp. 1–14.

[22] E. Arabi, B.C. Gruenwald, T. Yucelen, M.L. Fravolini, N.T. Nguyen, Model reference neuroadaptive control revisited: how to keep the system trajectories on a given compact set, in: AIAA Guidance, Navigation, and Control Conference, 2017, pp. 1–14.

[23] T. Yucelen, A.J. Calise, Robustness of a derivative-free adaptive control law, J. Guid. Control Dyn. 37 (5) (2014) 1583–1594, https://doi.org/10.2514/1.G000289.

[24] N.T. Nguyen, S.N. Balakrishnan, Bi-objective optimal control modification adaptive control for systems with input uncertainty, IEEE/CAA J. Autom. Sin. 1 (4) (2014) 423–434, https://doi.org/10.1109/JAS.2014.7004669.

[25] B. Gruenwald, T. Yucelen, On transient performance improvement of adaptive control architectures, Int. J. Control 88 (11) (2015) 2305–2315, https://doi.org/10.1109/JAS.2014.7004669.

[26] T. Yucelen, B.C. Gruenwald, J.A. Muse, A direct uncertainty minimization framework in model reference adaptive control, in: AIAA Guidance, Navigation, and Control Conference, 2015, pp. 1–13.

[27] Y. Song, Y. Wang, C. Wen, Adaptive fault-tolerant pi tracking control with guaranteed transient and steady-state performance, IEEE Trans. Autom. Control 62 (1) (2017) 481–487, https://doi.org/10.1109/TAC.2016.2554362.

[28] S. Boulouma, S. Labiod, H. Boubertakh, Linear adaptive actuator failure compensation for wing rock motion control, Aerosp. Sci. Technol. 67 (2017) 155–168, https://doi.org/10.1016/j.ast.2017.03.025.

[29] J. Yao, Z. Jiao, D. Ma, Adaptive robust control of DC motors with extended state observer, IEEE Trans. Ind. Electron. 61 (7) (2014) 3630–3637, https://doi.org/10.1109/TIE.2013.2281165.

[30] J. Cieslak, D. Efimov, D. Henry, Transient management of a supervisory fault-tolerant control scheme based on dwell-time conditions, Int. J. Adapt. Control Signal Process. 29 (1) (2015) 123–142, https://doi.org/10.1002/acs.2465.

[31] N.T. Nguyen, K.E. Hashemi, T. Yucelen, E. Arabi, Performance optimizing multi-objective adaptive control with time-varying reference model modification, in: AIAA Guidance, Navigation, and Control Conference, 2017, pp. 1–18.

[32] X. Bu, Y. Xiao, K. Wang, A prescribed performance control approach guaranteeing small overshoot for air-breathing hypersonic vehicles via neural approximation, Aerosp. Sci. Technol. 71 (2017) 485–498, https://doi.org/10.1016/j.ast.2017.10.005.

[33] X. Xu, L. Yang, J. Zhang, MRAC control with prior model knowledge for asymmetric damaged aircraft, Sci. World J. 2015 (2015) 247301, https://doi.org/10.1155/2015/247301.

[34] G.-D. Hu, M. Liu, The weighted logarithmic matrix norm and bounds of the matrix exponential, Linear Algebra Appl. 390 (2004) 145–154, https://doi.org/10.1016/j.laa.2004.04.015.

[35] J.A. Ouellette, Flight Dynamics and Maneuver Loads on a Commercial Aircraft with Discrete Source Damage, Ph.D. thesis, Virginia Polytechnic Institute and State University, 2010.